Physica C 470 (2010) 313–317

Contents lists available at ScienceDirect

Physica C

journal homepage: www.elsevier.com/locate/physc

Superconductivity of Ni-doping 2H–TaS$_2$

L.J. Li [a], X.D. Zhu [a,b], Y.P. Sun [a,b,*], H.C. Lei [a], B.S. Wang [a], S.B. Zhang [a], X.B. Zhu [a], Z.R. Yang [a], W.H. Song [a]

[a] *Key Laboratory of Materials Physics, Institute of Solid State Physics, Chinese Academy of Sciences, Hefei 230031, People's Republic of China*
[b] *High Magnetic Field Laboratory, Chinese Academy of Sciences, Hefei 230031, People's Republic of China*

ARTICLE INFO

Article history:
Received 20 November 2009
Accepted 16 January 2010
Available online 25 January 2010

Keywords:
Superconductivity
Single crystals
Charge density wave

ABSTRACT

The superconductivity of 2H–Ni$_x$TaS$_2$ single crystals with Ni-doping content of $0 \leqslant x \leqslant 0.08$ is investigated. Compared with the temperature dependence of resistivity $\rho(T)$ curve of un-doped 2H–TaS$_2$ with charge density wave (CDW) transition (T_{CDW} = 78 K), no sign of CDW is observed for Ni-doping sample Ni$_x$TaS$_2$, meaning the suppression of CDW caused by Ni-doping. The increase of superconducting critical temperature T_C caused by Ni-doping is observed and the optimal Ni-doping content corresponding to the maximum zero resistance temperature $T_{Czero}^{max} = 4.15$ K is $x = 0.04$. The superconductivity of Ni$_{0.04}$TaS$_2$ is investigated in detail. The obtained superconducting parameters indicated that Ni$_{0.04}$TaS$_2$ is an intermediate coupling anisotropic type-II superconductor with anisotropy ratio $\gamma = H_{c2}^{ab}(T)/H_{c2}^{c}(T) \approx 3.58$.

1. Introduction

Layered transition-metal dichalcogenides (TMDC's) of the type MX$_2$ (M is the transition metal, X = S, Se, Te) have been extensively studied for their rich electronic properties due to low dimensionality [1]. Each layer of TMDC's consists of a hexagonal transition metal sheet sandwiched by two similar chalcogen sheets, which can be regarded as stacking of covalent coupling X–M–X sandwiches, and the coupling between sandwiches being of weak van der Waals type. Charge density wave (CDW) and superconductivity coexist in most these materials such as 2H–TaSe$_2$, 2H–NbSe$_2$, 2H–TaS$_2$, 4Hb–TaS$_2$, and 4Hb–TaSe$_2$ [2–4]. The electron–phonon coupling and its relationship with the CDW have been investigated by angle resolved photoemission in 2H–TaSe$_2$ and 2H–NbSe$_2$ systems [5–7]. It is found that the CDW transition temperature decreases and meanwhile the superconducting critical temperature (T_C) increases, in TaSe$_2$ and TaS$_2$, which indicates that these two kinds of quantum orders (CDW and superconductivity) compete with each other [8–10]. CDW and superconductivity are two very different cooperative electronic phenomena, and yet both occur because of Fermi surface instabilities and electron–phonon coupling. CDW represents the periodic modulation of the charge density in solids, which is usually found in low-dimensional materials. 2H–TaS$_2$, a classic, layered TMDC, undergoes a CDW transition at ~78 K and a superconducting transition at ~0.8 K [1,2].

The intercalation effects in TaS$_2$ have attracted extensive efforts during the past decades [11–14]. With 3d-transitional metal (3d-TM) intercalation, enhancement of superconductivity and suppression of CDW has been observed in Fe$_{0.05}$TaS$_2$ [15], and copper intercalated Cu$_x$TaS$_2$ polycrystalline samples [16] and single crystals [17]. Very recently, the raise of T_C within low Ni-doping content Ni$_{0.05}$TaS$_2$ single crystals have been also observed [18]. In this paper, Ni$_x$TaS$_2$ single crystals with different Ni-doping content of $0 \leqslant x \leqslant 0.08$ are grown and their superconductivities are systemically investigated by the magnetic, electronic and heat transport experiments. For Ni$_{0.04}$TaS$_2$ single crystal with the maximum T_C its superconducting parameters are obtained.

2. Experimental

2H–Ni$_x$TaS$_2$ single crystals with x = 0, 0.02, 0.04, 0.05, 0.06, and 0.08 were grown using the NaCl/KCl flux method [19]. The room temperature crystal structure and lattice constants were determined by powder and single crystal X-ray diffraction (XRD) (Philips X'pert PRO) using Cu Kα radiation. To perform the powder XRD experiment, several single crystals were crushed to powder. Magnetization measurements were performed in a Quantum Design (QD) superconducting quantum interference device (SQUID) MPMS system ($1.8 \leqslant T \leqslant 400$ K, $0 \leqslant H \leqslant 5$ T). Resistivity measurements were carried out by the standard four-probe method in the temperature range of 1.8–300 K in a commercial QD Physical Property Measurement System (PPMS, $1.8 \leqslant T \leqslant 400$ K, $0 \leqslant H \leqslant 9$ T). Specific heat was measured by the thermal relaxation method (QD, PPMS) in the temperature range of 2–15 K.

---

[*] Corresponding author. Address: Key Laboratory of Materials Physics, Institute of Solid State Physics, Chinese Academy of Sciences, Hefei 230031, People's Republic of China. Tel.: +86 551 559 2757; fax: +86 551 559 1434.
E-mail address: ypsun@issp.ac.cn (Y.P. Sun).

0921-4534/$ - see front matter © 2010 Elsevier B.V. All rights reserved.
doi:10.1016/j.physc.2010.01.042

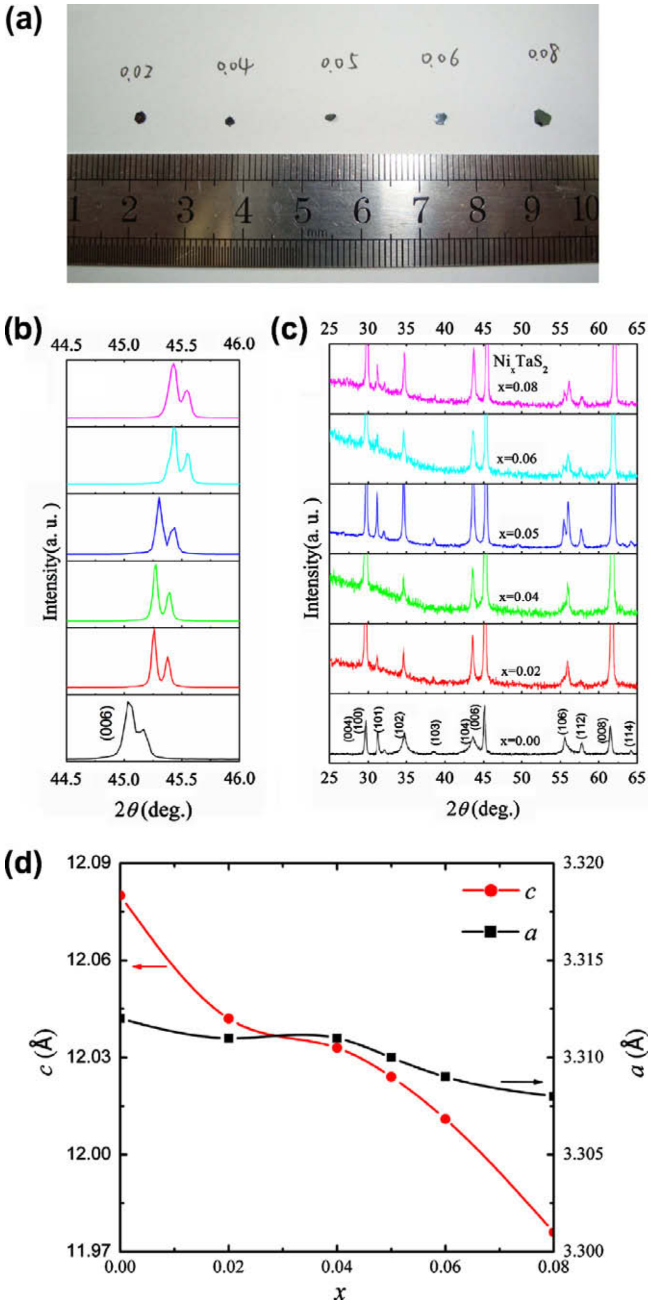

Fig. 1. (a) The photograph of Ni$_x$TaS$_2$ single crystals. (b) The magnification plot of (0 0 6) peak of Ni$_x$TaS$_2$ single crystals. (c) The powder XRD patterns of crushed single crystals. (d) The curve of the lattice constants a and c as a function of Ni-doping level in Ni$_x$TaS$_2$ single crystals.

3. Results and discussion

Fig. 1a[1] shows the typical single crystal photos. The grown crystals are dark blue, mirror-like plates with a typical size of 1.5 × 1.5 × 0.2 mm^3. The structures of the single crystals are determined by XRD pattern. The XRD patterns for Ni$_x$TaS$_2$ single crystals with x = 0, 0.02, 0.04, 0.05, 0.06, and 0.08 indicates that the orientations of the crystal surfaces are perpendicular to (0 0 1) plane. The magnified plot of (0 0 6) peak is displayed in Fig. 1b. Obviously, the (0 0 6) peak position shifts to high angle with increasing Ni-doping content, implying the decrease of the c-axis lattice constant. In order to obtain the lattice constants of Ni-doped samples, the powder XRD patterns of crushed single crystals are shown in Fig. 1c, and all the peaks can be well indexed to the 2H structure, meaning Ni-doping does not change the crystal structure of 2H–TaS$_2$. The lattice constants obtained by fitting powder XRD patterns are shown in Fig. 1d. It shows that the Ni-doping almost does not change the value of the lattice constant a, while it obviously reduces the lattice constant c. That is to say, the Ni-doping causes the shrinkage of the lattice along the c-axis direction, which is in contrast to the expansion of the lattice along c-axis direction caused by Cu-intercalation in Cu$_x$TaS$_2$ [16,17]. Considering the smaller ion radius of Ni compared with Ta ions, the reduction of lattice constant c suggests that Ni ions do not occupy the intercalation position S–Ta–S interlayer and but substitute on the position of Ta in S–Ta–S layer. The reason why Cu and Ni ions occupy different positions in 2H–TaS$_2$ lattice needs to be examined further.

In order to investigate the effect of Ni-doping on the CDW transition, the temperature dependence of the in-plane resistivity $\rho_{ab}(T)$ of Ni$_x$TaS$_2$ single crystals is measured. In Fig. 2a we plots the resistivity $\rho_{ab}(T)$ for Ni$_x$TaS$_2$ as a function of temperature under zero field in the temperature range of 2–280 K. It shows that $\rho_{ab}(T)$ almost follows a linear temperature dependence with no obvious change of curvature (like a kink) corresponding to the CDW transition observed in the high temperature region. That is to say, the CDW transition occurring at T_{CDW} = 78 K for 2H–TaS$_2$ is suppressed by Ni-doping, even if Ni-doping content is only 2%. Compared with

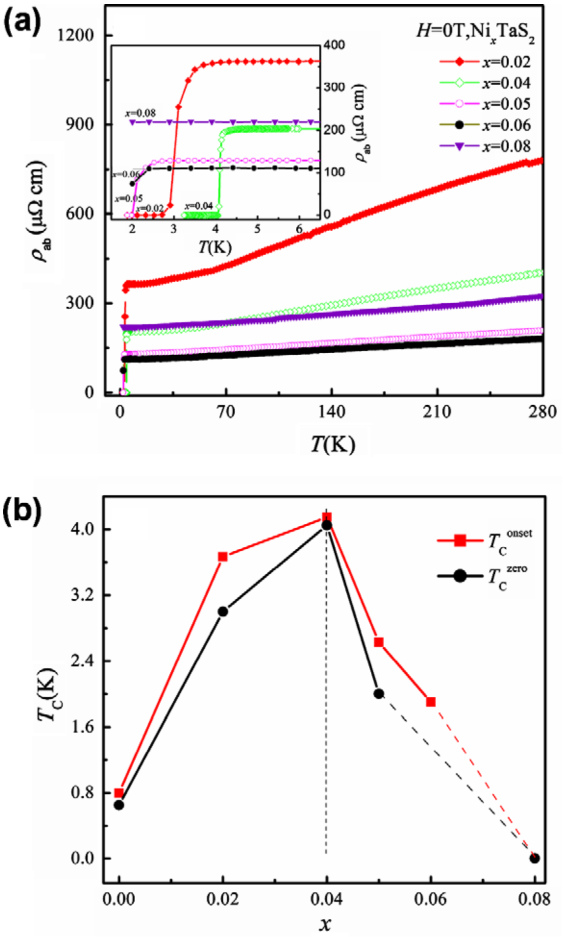

Fig. 2. (a) The temperature dependence of the resistivity $\rho_{ab}(T)$ for Ni$_x$aS$_2$. The inset shows the enlarged view of the low temperature part. (b) The Ni-doping level dependence of T_C^{onset} and T_C^{zero}.

---

[1] For interpretation of color in Figs. 1–7, the reader is referred to the web version of this article.